Low-energy reaction yields for $^{18}O(p,\gamma)$ and $^{18}O(\alpha,\gamma)$

R. B. Vogelaar, T. R. Wang, S. E. Kellogg, and R. W. Kavanagh
W. K. Kellogg Radiation Laboratory, California Institute of Technology, Pasadena, California 91125
(Received 16 October 1989)

Resonance yields, γ-ray branching, and low-energy limits have been measured for $^{18}O(p,\gamma)$ and $^{18}O(\alpha,\gamma)$, for $E_p < 0.22$ MeV and $E_\alpha < 0.78$ MeV, using a 4π array of NaI detectors. The results confirm previous resonance strengths, and set additional constraints on possible low-energy contributions to stellar reaction rates.

I. INTRODUCTION

As the hydrogen fuel is exhausted in stars burning in the catalytic CNO cycles, the core contracts and heats, and helium burning of the principal[1] residue, ^{14}N, produces ^{18}O via the sequence[2] $^{14}N(\alpha,\gamma)^{18}F(\beta^+\nu)^{18}O$, at temperatures $T \gtrsim 10^8$ K. The ^{18}O then reacts through $^{18}O(\alpha,n)^{21}Ne$ ($Q=-0.693$ MeV) and $^{18}O(\alpha,\gamma)^{22}Ne$ ($Q=9.669$ MeV); the (α,γ) reaction is dominant[3] for $T \lesssim 6\times10^8$ K, and may be important as a source of the high ^{22}Ne enrichment observed[4] in some meteorites. At higher temperatures, in quiescent or explosive nucleosynthesis, the neon isotopes are processed to heavier elements. In particular, the $^{22}Ne(\alpha,n)^{25}Mg$ reaction is the probable source[5] of neutrons to drive the *s*-process in massive ($M \gtrsim 2M_\odot$) stars.

Fifteen resonances in the $^{18}O(\alpha,\gamma)$ reaction have been reported[3] in the range $0.6 < E_\alpha < 2.3$ MeV. We have measured the lowest three of these (at $E_\alpha = 0.66$, 0.75, and 0.77 MeV), and determined upper limits for possible lower resonances corresponding to ^{22}Ne levels seen[6,7] in the $^{19}F(\alpha,p\gamma)^{22}Ne$ and $^{20}Ne(t,p)^{22}Ne$ reactions.

In addition, we have similarly measured the strengths of the lowest two known resonances in $^{18}O(p,\gamma)^{19}F$ ($Q=7.994$ MeV) and set upper limits at lower energies. The results are in agreement with prior work.[8] This reaction is weak compared to $^{18}O(p,\alpha)^{15}N$, but may lead to small leakage from the CNO cycle during hydrogen burning at $T \sim 10^8$ K.

II. EXPERIMENTAL METHOD

Several targets of Ta_2O_5 were prepared by anodic oxidation of 250 μm Ta discs, enriched to 97% in ^{18}O. Such targets are known[9] to be stoichiometrically Ta_2O_5 and to have an ^{18}O content about 0.25 $\mu g/cm^2$ times the anodizing volts; this we found to be consistent (to 10%) with observed energy-loss thicknesses from target profiles at the $E_p = 151$-keV resonance in $^{18}O(p,\gamma)$, for targets anodized to 25 V (see Fig. 1), 200 V, and 245 V. Since our determinations of resonance strengths use "thick-target" analysis,[10] only the stoichiometry is important here, along with the stopping power[11] (e.g., 160×10^{-15} eV cm^2 per Ta_2O_5 molecule at $E_p = 151$ keV).

Magnetically analyzed H_2^+ or α^+ beams were provided by the Caltech Pelletron accelerator, using the ion source in the HV terminal. Energy calibration for H_2^+ (±0.5 keV) via a temperature-stabilized Hall probe was based on $^{27}Al(p,\gamma)$ narrow resonances studied[12] during the previous year; α^+ energies (±1 keV) were from an NMR calibrated at the 606- and 1530-keV resonances[13,14] in $^{11}B(\alpha,n)$ and $^{24}Mg(\alpha,\gamma)$, respectively. The beam was defined by a circular 4-mm aperture about 1 m upstream from the target, which was clamped onto a circular knife-edge at the end of the beam line. The beam-line vacuum was $<7\times10^{-7}$ torr. To withstand beam currents up to 50 μA, the back of the target was directly water-cooled, using gravity flow between insulated reservoirs. For the thickest target (anodized to 245 V), proton-resonance profiles before and after a 0.5-Coulomb run with 650-keV α^+ revealed a 12% decrease in step height and reduction from 65 to 43 keV in width of the flat-topped region but no change in width at half-maximum, suggesting centralized sputtering loss of Ta_2O_5 with extra loss of oxygen by dissociation.

To facilitate resonance profiling, the target assembly was connected to a power supply that was varied from 0 to 20 kV in a linear sawtooth pattern with a 40-sec period. The entire system was electrically insulated and returned to ground through an Ortec current integrator for beam-charge measurement.

Gamma-rays from the targets were observed in 4π geometry with four $15\times15\times25$-cm^3 rectangular NaI scintillators stacked symmetrically around the target, leaving a $2.5\times2.5\times25$-cm^3 rectangular channel for the final segment of beam pipe. For background reduction, cosmic-ray-veto paddles were placed around the detectors, and the assembly was surrounded by 5-cm Pb and 20 cm of paraffin. Data were stored in a computer in "event mode," an event consisting of pulse heights from each of the four NaI (1024 channels), and the digitized ramp voltage (256 channels, calibrated separately for voltage versus channel). Current-integrator pulses and a standard pulser (at 20 Hz) were also binned with the ramp voltage, to monitor possible corona or other current leakage (always negligible) and dead-time losses ($\lesssim 5\%$). To reduce the storage of extraneous background events, hardware thresholds were imposed, requiring either that one detector have >2.7 MeV deposited (i.e., above the Th background γ-ray) or that two detectors have >200 keV each (anticipating γ-ray cascades). The background event-storage rate was thus reduced to about

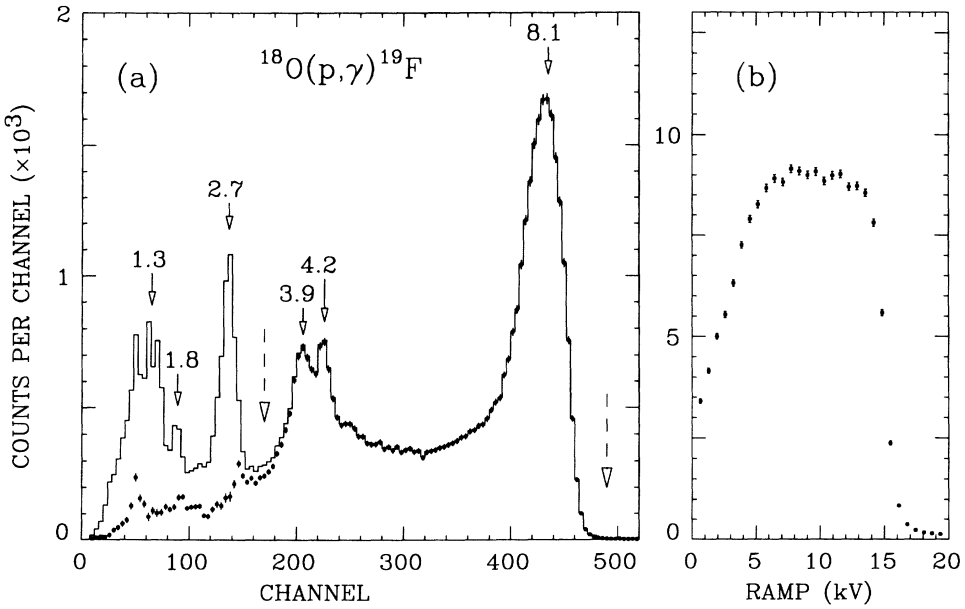

FIG. 1. (a) The $^{18}O(p,\gamma)$ total-energy spectrum from the 4π NaI array, with and without background subtraction, obtained with H_2^+ beam while ramping the target potential over the resonance at $E_p = 150.5$ keV. Peaks are labeled in MeV; those at 3.9 and 4.2 MeV are expected from the known cascades (Ref. 8) from the resonant level at 8.137 MeV in ^{19}F. (b) The yield versus target potential, for the spectrum region between channels 170 and 490 [dashed arrows in (a)], from which the resonance energy and strength are determined; the ordinate-scale unit is 10^3 counts per 0.62 keV.

5 sec^{-1}. The stored data were processed later with various energy cuts and coincidence requirements to optimize signal-to-background ratios and to determine cascade schemes.

Two-dimensional spectra of ramp voltage versus the total energy deposited were also collected, allowing online display of excitation functions with selectable total-energy windows.

The detection efficiencies were determined, for the cuts used, by Monte Carlo calculations, using the Electron-Gamma Shower code EGS4[15] applied to our geometry. The calculated efficiencies agreed well (±5%) with test runs on several resonances in $^{27}Al(p,\gamma)$ having well-known strengths and cascade branching, and with a calibrated ^{24}Na source, as described elsewhere.[12] (The present experiment exploited the detection system, outlined above, which had been developed[12] for a previous experiment.)

III. RESULTS

$^{18}O(p,\gamma)$. Figure 1 shows the data obtained from a thin target bombarded with 316-keV H_2^+ while ramping the target potential between 0 and +20 kV to sweep over the 151-keV resonance. Figure 1(a) is the pulse-height spectrum of the summed pulses from the four detectors, with and without time-dependent background subtraction. The background below channel 150 is from the usual ^{40}K and Th lines, and from ^{22}Na and ^{26}Al target-chamber contamination that occurred during prior experiments with radioactive targets of those isotopes. The peak at 8.1 MeV corresponds to the excitation energy (8.137 MeV) in ^{19}F, comprising the transition directly to the ground state plus summing of the numerous cascades. The peaks at 3.9 and 4.2 MeV are due to the dominant[8] cascades through the 3.908-MeV level in ^{19}F. Figure 1(b) shows the yield versus ramp voltage for spectrum pulses within a window between channel 170 and 490 (3 to 8.5 MeV). From the height of the yield curve (9000 counts per channel), the calculated efficiency (0.85±0.05) for the window, and the charge (29.2 mC of H_2^+), the resonance strength is found to be 0.92±0.06 meV. The low-energy edge of the resonance profile (note that reaction energy *decreases* with ramp voltage) determines the resonance energy to be 150.5±0.5 keV and the width $\Gamma < 0.5$ keV.

A similar run on the same target with 446-keV H_2^+ beam energy, thus ramping through the much weaker $E_p = 215$-keV resonance, was taken for a total charge of 80.4 mC. The γ-ray energy window was narrowed to 6.4–8.9 MeV in order to exclude a $^{19}F(p,\alpha\gamma)$ contaminant peak (6.1 MeV) about twice as strong as the $^{18}O(p,\gamma)$ full-energy peak (8.2 MeV). The resonance profile was clearly defined on a background level about equal to the resonance step height. By imposing various coincidence requirements on the event record, the principal cascades were extracted as follows: 39±5% to the lowest three (unresolved) levels of ^{19}F below $E_x = 200$ keV; 44±5% to $E_x = 1.35$ MeV; and 17±5% to $E_x = 3.91 \pm 0.10$ MeV. The resonance strength was determined from the step height by comparison with that from the 151-keV resonance using the same γ-ray energy window, giving $\omega\gamma = 5.0 \pm 1.0$ μeV; the error includes uncertainty in the relative efficiency due to branching. From the resonance edge the resonance energy is found to be 214.7±0.5 keV.

A longer run (2.9 h; 400 mC) on the thickest target ($\Delta E_p = 70$ keV per 151-keV resonance profiling before and after), with the ramped 250-keV H_2^+ beam and the 6.4–8.9-MeV γ-ray window, had a yield essentially at the background level (59±46 net counts). From this, assum-

TABLE I. Resonance parameters for $^{18}O(p,\gamma)^{19}F$. Values in brackets are from Ref. 8. $\omega\gamma$ in c.m. system, Γ in lab.

E_p (keV)	$\omega\gamma$ (μeV)	Γ (keV)	$^{19}F^*$ (keV)
214.7±0.5	5.0±1.0	<0.8	8197.5[c]
[216±1]	[≥8][a]	[≤1]	
150.5±5	920±60	<0.5	8136.7
[151±2]	[1000±100]	[≤0.3]	
50–120	<(0.02±0.02)		<8108
[95±3]	[≤0.05][b]		

[a]From yield of secondary transitions only.
[b]From yield of 197-keV γ-ray at 0°, assuming 100% branching.
[c]Principal branches (%) to E_x (keV): 39±5 to 0–200; 44±5 to 1346; 17±5 to 3908±100.

ing cascading as at $E_p=151$ keV, we find $\omega\gamma<(0.02\pm0.02)$ μeV for $E_p\approx120$ keV, decreasing for lower E_p, through the energy and energy-loss dependence of the yield expression, to $<(0.01\pm0.01)$ μeV at $E_p=50$ keV. (Additional uncertainty due to efficiency variation with branching is less than ±20% for the extreme assumptions of all transitions directly to ground versus all triple cascade.) The results, summarized in Table I, are in good agreement with those of Wiescher *et al.*[8]

$^{18}O(\alpha,\gamma)$. Figure 2 shows data obtained from the thickest target ($\Delta E_\alpha=175$ keV) bombarded with 80.8 mC of 779-keV α^+ and ramped to sweep over the 770-keV resonance. As above, Fig. 2(a) is the combined spectrum from the four detectors and Fig. 2(b) gives the yield versus ramp voltage, for the spectrum window between channels 232 and 600 (4.4–11.1 MeV; 76% efficiency). From the step height and position, the resonance strength is $\omega\gamma=1.20\pm0.12$ meV and the resonance energy is 767.6±1.0 keV. The plateau at higher ramp voltage (lower E_α) is due to the yield from two lower resonances, which are also integrated since the target thickness is about 175 keV. By subtracting the spectrum of events with the higher ramp voltage from the spectrum with lower voltage (both normalized to the same beam charge), an event file was formed for the 767.6-keV resonance only. Then imposing various coincidence requirements, the γ-ray branching from the resonance level could be deduced, using known[16] values for subsequent branching of lower levels. The results are shown in Table II. Figure 3 shows the spectrum and excitation function for the weakest observed resonance, at $E_\alpha=662.1$ keV. Here a narrower spectrum window was set to exclude lower-energy background from neutrons. The branching was determined as above (in good agreement with Ref. 17), and the efficiency deduced to be 57%. These results and those from a third resonance at 749.9 keV are also included in Table II. They are in fair agreement with those of Trautvetter *et al.*[3]

A search was made for possible still lower resonances by taking long runs (~0.5 C) at lower E_α. The γ-ray spectrum from one such run is shown in Fig. 4, for $E_\alpha=650$ keV. The excess counts (over background) near channel 350 are attributed almost entirely to capture in NaI of neutrons produced from $^{11}B(\alpha,n)$ at the known[13] narrow resonance at $E_\alpha=606$ keV ($\omega\gamma\approx0.2$ eV); the excess near channel 600 is due to $^{11}B(\alpha,\gamma)$ from the same resonance ($\omega\gamma\approx0.02$ eV). The ^{11}B contaminant was identified from its well-known[13] (α,γ) cascade structure

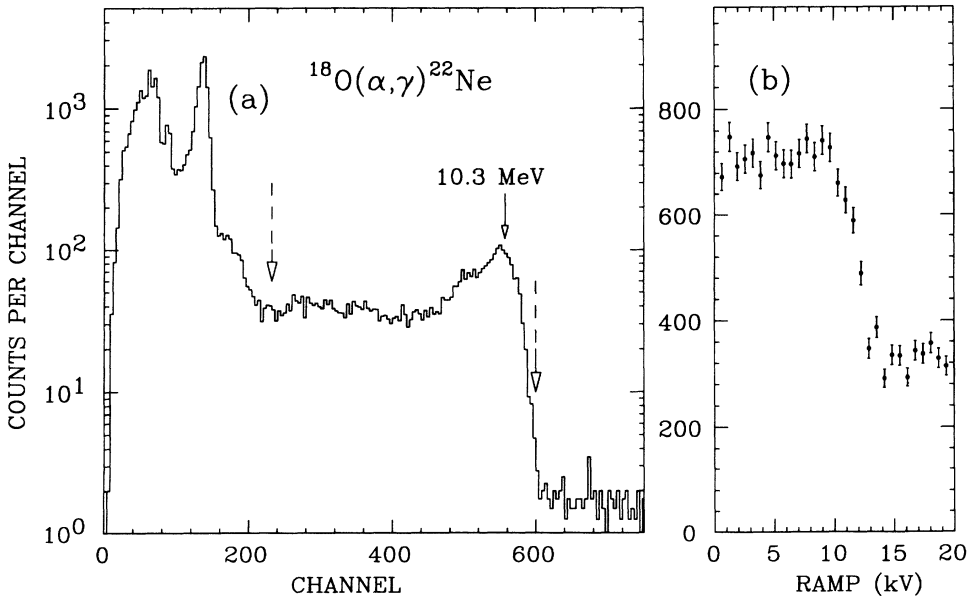

FIG. 2. As in Fig. 1, but with α^+ beam and a thicker target. (a) The $^{18}O(\alpha,\gamma)$ spectrum obtained while ramping over the resonance at $E_\alpha=767.6$ keV and (b) the yield versus target potential for the spectrum window between channels 232 and 600.

TABLE II. Resonance parameters for $^{18}O(\alpha,\gamma)^{22}Ne$. Values in brackets are from Ref. 3. $\omega\gamma$ in c.m. system.

E_α (keV)	$\omega\gamma$ (μeV)	Γ (lab) (keV)	$^{22}Ne^*$ (keV)	γ Branch (%) $0(0^+)$	$1.27(2^+)$	$4.46(2^+)$	$5.34(1^+)$	$6.85(1^+)$	$7.49(1^-)$
767.6±1.0	1200±120	<1.7	10297.3	<4	57±7	6±2	17±4	9±3	11±3
[769±4]	[>670]	[≤1.5]			[60]				
749.9±1.0	560±60	<1.7	10282.7	<6	25±5	1	44±5	20±4	10±3
[755±4]	[470±80]	[≤2]			[30±4]		[55±4]	[15±4]	
662.1±1.0	230±25	<2	10211.0[a]	83±5	17±5		Σ<4		
[656±4]	[290±50]	[≤5]		[77±5]	[23±5]				
≤640	<(2.0±0.5)		≤10193						
≤560	<(0.0±0.2)		≤10127						

[a] $J^\pi = 1^-$ (Ref. 17).

via the event record; the neutron response of the NaI system was determined with a weak ^{252}Cf neutron source at the target position. The excess for the $^{18}O(\alpha,\gamma)$ peak region between channels 450 and 600 [cf. Fig. 2(a)] is 99±30 counts, nearly all attributable to the ^{11}B contamination. The detection efficiency for this window was calculated[15] for various cascades, giving 57, 53, 37, and 31%, respectively, for resonance directly to ground ($R \rightarrow 0$), ($R \rightarrow 1.27 \rightarrow 0$), ($R \rightarrow 5.34 \rightarrow 0$), and ($R \rightarrow 6.12 \rightarrow 1.27 \rightarrow 0$). Taking 50±10% as a reasonable efficiency estimate, and 99 counts as a conservative upper limit, gives $\omega\gamma < (2.0\pm0.5)$ μeV for $640 > E_\alpha > 465$ keV.

Another run (0.44 C), taken with a third target (120 keV thick) at $E_\alpha = 565$ keV (below the ^{11}B resonance), was indistinguishable from background above channel 250; between channel 450 and 600, the excess was 4±26 counts. With the (50±10)% detection efficiency for this window, this excess sets an upper limit for resonances down to $E_\alpha \approx 440$ keV, viz., $\omega\gamma < (0.0\pm0.2)$ μeV. This limit applies in particular to the possible resonance at 534±24 keV corresponding to the ^{22}Ne level at 10.105 MeV reported by Broude *et al.*[6] from $^{19}F(\alpha,p\gamma\gamma)^{22}Ne$. The possible resonance at $E_\alpha = 566\pm18$ keV, due to the level at 10.132 MeV seen by Flynn *et al.*[7] in $^{20}Ne(t,p)^{22}Ne$, might lie above the energy range spanned by this target, in which case the strength limit 2 μeV from the previous run is applicable. In view of the cited energy uncertainties, the two reports may well correspond to the *same* level, at a weighted mean energy $E_\alpha = 546\pm14$ keV.

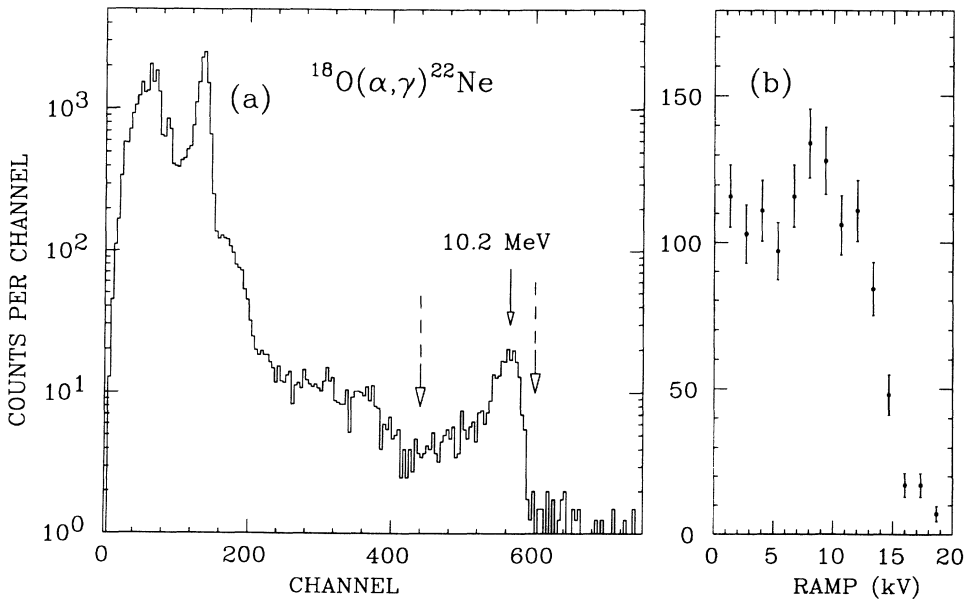

FIG. 3. As in Fig. 2, for the resonance at 662.1 keV. The low-energy window level was raised to exclude contaminant yield from neutrons. In (b) the ordinate-scale unit is counts per 1.25 keV.

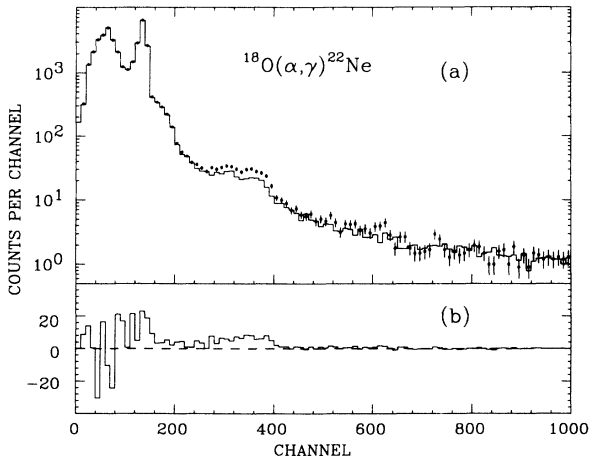

FIG. 4. As in Fig. 2(a), with $E_\alpha = 650$ keV. The $^{18}O+\alpha$ data (points) and room background (histogram) are shown, and their difference (lower histogram). The excess is due to $^{11}B(\alpha,n)$ and $^{11}B(\alpha,\gamma)$ from boron contamination in the target.

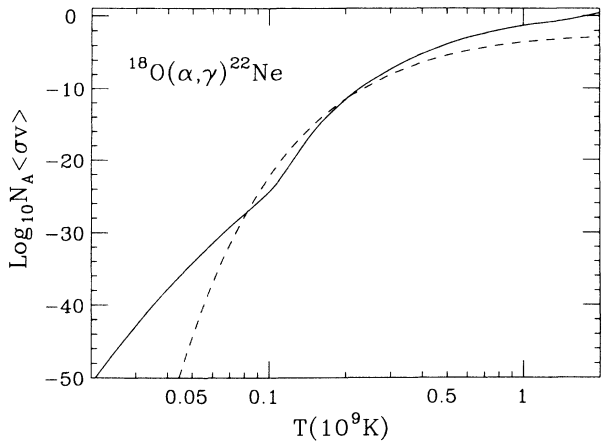

FIG. 5. The $^{18}O(\alpha,\gamma)$ reaction rate, $N_A\langle\sigma v\rangle$ in units of $cm^3\,sec^{-1}\,mole^{-1}$, versus temperature. The solid curve is from Table V of Ref. 3, and includes all known resonances plus nonresonant direct capture. The dashed curve shows the *additional* rate contribution that would result from inclusion of a resonance at $E_\alpha = 546$ keV with the present strength limit, taken as $\omega\gamma = 0.2\,\mu$eV

IV. CONCLUSION

The parameters we find for the lowest two known resonances in $^{18}O(p,\gamma)$ and the lowest three in $^{18}O(\alpha,\gamma)$ are in reasonable agreement with earlier[3,8] values, so that the previous results for stellar reaction rates are not significantly altered. For $^{18}O(\alpha,\gamma)$, the contribution to the reaction rate,[18] $N_A\langle\sigma v\rangle$, from a resonance at $E_\alpha = 546$ keV with our upper-limit strength, $\omega\gamma = 0.2\,\mu$ eV, is illustrated in Fig. 5 in comparison with the total rate[3] from higher resonances plus direct capture. It is evident that the contribution could still dominate the rate for $0.08 \lesssim T_9 \lesssim 0.2$. The same strength for lower hypothetical resonance energy greatly increases the rates at low T_9, as can be roughly visualized by translating the dashed curve in Fig. 4 to lower temperatures in proportion to the resonance-energy decrease.

ACKNOWLEDGMENTS

This work was supported by the National Science Foundation Grant No. PHY88-17296.

[1]E. M. Burbidge, G. R. Burbidge, W. A. Fowler, and F. Hoyle, Rev. Mod. Phys. **29**, 547 (1957).
[2]R. G. Couch, H. Spinka, T. A. Tombrello, and T. A. Weaver, Astrophys. J. **172**, 395 (1972).
[3]H. P. Trautvetter, M. Wiescher, K.-U. Kettner, C. Rolfs, and J. W. Hammer, Nucl. Phys. **A297**, 489 (1978).
[4]D. C. Black, Geochim. Cosmochim. Acta **36**, 347 (1972).
[5]J. W. Truran and I. Iben, Astrophys. J. **216**, 797 (1977).
[6]C. Broude, W. G. Davies, J. S. Forster, and G. C. Ball, Phys. Rev. C **13**, 953 (1976).
[7]E. R. Flynn, Ole Hansen, and O. Nathan, Nucl. Phys. **A228**, 189 (1974).
[8]M. Wiescher, H. W. Becker, J. Gorres, K.-U. Kettner, H. P. Trautvetter, W. E. Kieser, C. Rolfs, R. E. Azuma, K. P. Jackson, and J. W. Hammer, Nucl. Phys. **A349**, 165 (1980).
[9]D. Phillips and J. P. S. Pringle, Nucl. Instrum. Methods **135**, 389 (1976).
[10]D. G. Sargood, Phys. Rep. **93**, 61 (1982).
[11]H. H. Anderson and J. F. Ziegler, *Hydrogen Stopping Powers and Ranges in All Elements* (Pergamon, New York, 1977).
[12]R. B. Vogelaar, Ph.D. Thesis, California Institute of Technology, 1989; R. B. Vogelaar *et al.* (unpublished).
[13]T. R. Wang, R. B. Vogelaar, and R. W. Kavanagh, Bull. Am. Phys. Soc. **33**, 1563 (1988), and (to be published).
[14]J. W. Maas, A. J. C. D. Holvast, A. Baghus, H. J. M. Aarts, and P. M. Endt, Nucl. Phys. **A301**, 237 (1978).
[15]W. R. Nelson, H. Hirayama, and D. O. Rogers, SLAC Report 265, 1985.
[16]P. M. Endt and C. Van der Leun, Nucl. Phys. **A310**, 1 (1978).
[17]U. E. P. Berg and K. Wienhard, Nucl. Phys. **A318**, 453 (1979).
[18]W. A. Fowler, G. R. Caughlan, and B. A. Zimmerman, Annu. Rev. Astron. Astrophys. **13**, 69 (1975).